Applied and Environmental Microbiology, Apr. 2011, p. 2685–2694 Vol. 77, No. 8
0099-2240/11/$12.00 doi:10.1128/AEM.02459-10

Geomicrobiology of La Zarza-Perrunal Acid Mine Effluent (Iberian Pyritic Belt, Spain)▽†

Elena González-Toril,[1]* Ángeles Aguilera,[1] Virginia Souza-Egipsy,[1] Enrique López Pamo,[2] Javier Sánchez España,[2] and Ricardo Amils[1,3]

Centro de Astrobiología (INTA-CSIC), Carretera de Ajalvir km 4, Torrejón de Ardoz, 28850 Madrid, Spain[1]; Instituto Geológico y Minero de España, 28003 Madrid, Spain[2]; and Centro de Biología Molecular Severo Ochoa (UAM-CSIC), Universidad Autónoma de Madrid, Cantoblanco, 28049 Madrid, Spain[3]

Received 18 October 2010/Accepted 17 February 2011

Effluent from La Zarza-Perrunal, a mine on the Iberian Pyrite Belt, was chosen to be geomicrobiologically characterized along a 1,200-m stream length. The pH at the origin was 3.1, which decreased to 1.9 at the final downstream sampling site. The total iron concentration showed variations along the effluent, resulting from (i) significant hydrolysis and precipitation of Fe(III) (especially along the first reach of the stream) and (ii) concentration induced by evaporation (mostly in the last reach). A dramatic increase in iron oxidation was observed along the course of the effluent [from $Fe(III)/Fe_{total} = 0.11$ in the origin to $Fe(III)/Fe_{total} = 0.99$ at the last sampling station]. A change in the O_2 content along the effluent, from nearly anoxic at the origin to saturation with oxygen at the last sampling site, was also observed. Prokaryotic and eukaryotic diversity throughout the effluent was determined by microscopy and 16S rRNA gene cloning and sequencing. Sulfate-reducing bacteria (*Desulfosporosinus* and *Syntrophobacter*) were detected only near the origin. Some iron-reducing bacteria (*Acidiphilium*, *Acidobacterium*, and *Acidosphaera*) were found throughout the river. Iron-oxidizing microorganisms (*Leptospirillum* spp., *Acidithiobacillus ferrooxidans*, and *Thermoplasmata*) were increasingly detected downstream. Changes in eukaryotic diversity were also remarkable. Algae, especially *Chlorella*, were present at the origin, forming continuous, green, macroscopic biofilms, subsequently replaced further downstream by sporadic *Zygnematales* filaments. Taking into consideration the characteristics of this acidic extreme environment and the physiological properties and spatial distribution of the identified microorganisms, a geomicrobiological model of this ecosystem is advanced.

The peculiar ecology and physiology of extremophiles and the environments in which they develop have intrigued microbiologists since their discovery. The biotechnological potential of their unusual properties make their study of great interest (32, 34, 37, 41).

Environments with extremely low pH values do not abound. They are mainly associated with two phenomena: volcanic and hydrothermal activities (hot sulfur springs, mud spots, etc.) and metal mining activities (16). The second category is especially interesting, because, in general, the extreme low pH of the habitat is a consequence of microbial metabolism (18) and not a condition imposed by the system, as is the case in many other extreme environments (e.g., high temperature, ionic strength, radiation, and pressure). Acidophilic chemolithotrophic microorganisms present in these environments have the potential to accelerate the oxidation and dissolution reactions of metal sulfides, resulting in acidic waters with high concentrations of sulfate and heavy metals (35).

These acidic waters are known as acid mine drainage (AMD), and they are a serious environmental problem in the province of Huelva (southwestern Spain). These acidic solutions emerge from mine portals, waste-rock piles, and/or tailings from ponds in the massive sulfide mines of the Iberian Pyrite Belt (IPB), transporting large amounts of acidity, dissolved sulfates, and soluble metals (44, 45, 51).

Although the geomicrobiology of AMD in the Iberian Pyrite Belt has been studied at length (17, 18, 40, 49), our knowledge of the microorganisms involved in iron and sulfur metabolism is far from complete. Most of the studies have been focused on iron and sulfur biological oxidation, but little is known about iron and sulfur biological reduction in AMD. Gathering information about the operation of these activities is fundamental to the development of efficient biotechnological processes such as biomining or AMD bioremediation.

La Zarza-Perrunal effluent represents an excellent model for the study of iron and sulfur metabolism, because a complete transition of these elements can be observed in less than a 2-km stream length in the mine. Although it finally closed in the 1990s, La Zarza-Perrunal site (Huelva, Spain) was mined in pre-Roman and Roman times for the recovery of Ag and Au and, in modern times, for sulfuric acid and metal retrieval (Cu, Zn, and Pb) (36). This acid effluent flows at a fairly constant rate along 2.6 km (43). After receiving some fresh water, this stream meets the Tamujoso creek and, finally, the Tallisca creek, where it is ultimately neutralized. Previous studies have addressed the geochemical evolution of this site (43), but a correlation with the associated microorganisms was needed to understand the geomicrobiology of the system.

There are two clearly differentiated sets of conditions in this effluent: (i) near the portal in which dissolved iron is mainly

* Corresponding author. Mailing address: Centro de Astrobiología (INTA-CSIC), Carretera de Ajalvir km 4, Torrejón de Ardoz, 28850 Madrid, Spain. Phone: 34-915206461. Fax: 34-915207074. E-mail: etoril@cbm.uam.es.

† Supplemental material for this article may be found at http://aem.asm.org/.

▽ Published ahead of print on 25 February 2011.

reduced and the oxygen concentration is rather low and (ii) 1,200 m downstream, where iron is completely oxidized and dissolved oxygen (DO) is near saturation. Also, there is a very clear eukaryotic microbial correlation; the stream bed of the effluent is coated by a continuous photosynthetic biofilm along the first meters, and the biofilm disappears as soon as the concentration of oxidized iron increases.

This study analyzed the microbial diversity of this area in relation to the physical and chemical conditions of the effluent. In order to achieve this goal, several methods were used, including conventional techniques involving species identification based on morphological and morphometric criteria to identify eukaryotes and molecular techniques, such as gene cloning, to characterize prokaryotic diversity. In addition, the structural features of natural phototrophic biofilms were also analyzed by transmitted light and scanning electron microscopy in backscattered electron mode (SEM-BSE).

MATERIALS AND METHODS

Study site and environmental conditions. Following a preliminary geochemical characterization of La Zarza-Perrunal mine effluent (43), field work was carried out in May 2007 under low-flow hydrologic conditions. To determine the geomicrobiological transition of the acid waters, three sampling points were established at increasing distances from their respective discharge points: *LZ1*, an iron-reduced station (20 m downstream from the mine portal); *LZ2*, a transition station (1,000 m downstream); and *LZ3*, where iron is completely oxidized (1,200 m downstream) (see Fig. S1 in the supplemental material). Water samples were taken with 60-ml syringes and Millipore sampling equipment, subjected to filtration through 0.45-μm-pore-size membrane filters on site, acidified to pH <2 with HNO_3, and stored in 125-ml polyethylene bottles at 4°C.

Field parameters such as pH, E_h, temperature, dissolved oxygen level, and electric conductivity were measured *in situ* with Hanna portable instruments properly calibrated against calibration standards. Flow rates were measured with digital flow meters (Global Water). A semiquantitative estimation of Fe(II) concentrations was performed *in situ* with Merckoquant (Merck) strips. A more precise iron species identification was performed by colorimetric digital titration (Hach) using citrate as solution buffer, sodium periodate as an Fe(II) oxidant, and sulfosalicylic acid as an Fe(III) colorimetric detector. The accuracy of this method, calculated by repeated analyses of internal standards, was ±1% in the 100 to 1,000 mg/liter Fe_t range, ±4% in the 50 to 100 mg/liter Fe_t range, and ±12% in the 10 to 50 mg/liter Fe_t range.

Analytical procedures. Water samples were analyzed by atomic absorption spectrometry (AAS) for Na, K, Mg, Ca, Fe, Cu, Mn, Zn and Al content, by inductively coupled plasma atomic emission spectrometry (ICP-AES) for Ni content, and by inductively coupled plasma mass spectrometry (ICP-MS) for As, Cd, Co, Cr, and Pb content. Sulfate was gravimetrically measured as $BaSO_4$. The accuracy of the analytical methods was verified against certified reference waters, and close agreement with certified values was achieved for all metals. ^{115}In was used as an internal standard for calibration of the ICP-MS analyses. The detection limits for trace elements were 10 μg/liter for Zn, 2 μg/liter for Ni, Co, Cr, and Pb, and 0.4 μg/liter for As, Cd, and Cu. The detection limit for the major cations Na, K, Ca, Mg, Mn, Fe, and Al was <1 mg/liter in all cases.

Biofilm sample collection. Photosynthetic biofilm samples were collected from the three sampling stations. Samples for DNA extraction were collected with sterile pipettes and stored at −20°C until further processing. Samples for scanning electron microscopy were secured for transport with a thin layer of alginic acid (1%), which gelled in place on the biofilm surface after the addition of $CaCl_2$ (1%). Samples were fixed in the field with 2.5% glutaraldehyde in acid sterile distilled water (pH 2). Samples were kept cold (5°C) and dark until further processing.

Microscopy and morphotype identification. Identification of algae and heterotrophic protists was carried out to the lowest possible taxonomic level by direct microscopic observation of different phenotypic features based on previous studies of the eukaryotic communities in acid environments (2, 3, 4, 5, 6, 29) as well as by the use of identification keys for algae (10), freshwater plankton (13), protozoa (26), euglenoid flagellates (27), *Euglenophyta* (50), *Protoctista* (33), and diatoms (39). A Zeiss Axioscope 2 phase-contrast microscope was used in this work.

DNA extraction, PCR amplification, and sequencing. A Fast DNA spin kit for soil (Q-Bio Gene Inc.) was used for DNA extraction from water, sediment, and biofilm samples according to the manufacturer's instructions. Pelleted microorganisms from water samples, sediments, and biofilms were washed five times with acid sterile and filtered water (pH 1) and once with phosphate-buffered saline (PBS) (130 mM sodium chloride, 10 mM sodium phosphate buffer; pH 7.2) prior to DNA extraction. DNA was purified by passage through a GeneClean Turbo column (Q-Bio Gene Inc.) and quantified by ethidium bromide-UV detection using an agarose gel. The 16S rRNA genes from bacteria, archaea, and eukaryotic plastids were amplified by PCR in mixtures containing 2 to 3 ng of DNA per 50-μl reaction volume, 1× PCR buffer (Promega Biotech Iberica, Spain), 250 μM (each) deoxynucleotides (Amersham Biosciences, United Kingdom), 2.5 mM $MgCl_2$, 100 μg/ml bovine serum albumin (BSA), 0.5 μM each forward and reverse primer, and 2.5 U of *Taq* DNA polymerase (Promega Biotech Iberica, Spain). In the amplification reactions, the reverse primer was 1492r (5′-TACC TTGTTACGACTT-3′) (1), and the forward primer was either *Bacteria*-specific 27f (5′-AGAGTTTGATCCTGGCTCAG-3′) (25) or *Archaea*-specific 21f (5′-T TCCGGTTGATCCYGCCGGA-3′) (14). PCR conditions were as follows: initial denaturation at 94°C for 5 min, followed by 30 cycles of denaturation at 94°C for 40 s, annealing at 52°C for 1 min for *Bacteria* amplification and at 56°C for 1 min for *Archaea* amplification, and extension at 72°C for 1 min.

PCR amplifications of 16S rRNA genes were purified using a GeneClean Turbo column (Q-Bio Gene Inc.) and cloned using a Topo TA cloning kit (Invitrogen). The PCR products were directly sequenced using a BigDye sequencing kit (Applied Biosystems) according to the manufacturer's instructions.

Phylogenetic analysis. Sequences were analyzed using BLAST at the NCBI database (http://blast.ncbi.nlm.nih.gov/Blast.cgi). Sequences were also checked for potential chimeras by the use of the Bellerophon Chimera Check program (22) and Mallard program (8) and were subsequently added to the most important BLAST hits to create a database of over 50,000 homologous prokaryotic 16S rRNA primary sequences by using the ARB software package aligning tool (30) (http://www.arb-home.de). The rRNA alignment was corrected manually, and alignment uncertainties were omitted. Only unambiguously aligned positions were used to construct phylogenetic trees with ARB. Phylogenetic trees were generated using parsimony and neighbor joining with a subset of 100 nearly full-length (>1,400 bp) sequences. Filters which excluded highly variable positions were used.

Scanning electron microscopy in backscattered electron detection mode (SEM-BSE). The internal structures of the microbial communities that form the biofilms covering the stream substrate at the selected sites were studied by SEM-BSE. Three different types of samples were collected from each main section of the stream: one covered with green biofilms, a second covered with filamentous biofilms, and a third mostly free of biofilms. The field-fixed samples were washed in the laboratory with acid sterile distilled water and postfixed with 1% osmium tetroxide–distilled water for a minimum of 8 h. Samples were dehydrated using an ascending (30, 50, 70, 90, and 100%) series of ethanol concentrations and then subjected to infiltration with LR-White resin for 24 h. Infiltrated samples were polymerized at 65°C for 24 h. Once polymerized, the blocks were cut transversally using a diamond saw, finely polished, and coated with carbon following the protocols of Ascaso and Wierzchos (7) and Wierzchos and Ascaso (54) and examined under a scanning electron microscope with a backscattered electron (BSE) detector plus an auxiliary X-ray energy-dispersive spectroscopy (EDS) microanalytical system. Transverse sections of the polished surfaces of the rocks were examined using a Jeol 5600LV SEM equipped with a BSE detector and an INCA Oxford microanalytical EDS system. EDS operating conditions were as follows: 0° tilt angle, 35° take-off angle (EDS), 15-kV acceleration potential, and 10- or 20 (EDS)-mm working distance.

Nucleotide sequence accession numbers. Sequences obtained in this study have been deposited in the EMBL sequence database under accession numbers from HM745403 to HM745467.

RESULTS

Geochemical parameters. Sample locations were chosen to cover most of the area under study, and a complete range of the different microbial assemblages was observed. The AMD was monitored at three sampling stations: *LZ1*, located 20 m downstream from the mine portal, and *LZ2* and *LZ3*, located 1,000 and 1,200 m downstream from the mine portal, respectively (see Fig. S1 in the supplemental material). The geochemical characteristics observed for the different sampling stations,

TABLE 1. Physicochemical data, iron species identification, and major ion concentrations in water samples from the three sampling stations along La Zarza-Perrunal effluent[a]

Sample	Distance from origin (m)	Digital location[b]	Field data						Iron species identification				SO_4^{2-} (mM)
			pH	E_h (mV)	EC (mS/cm)	T (°C)	DO (mg/liter)	DO (%)	Fe_t (mM)	Fe^{2+} (mM)	Fe^{3+} (mM)	Fe^{2+}/Fe_t (%)	
LZ1	20	159470, 4180430	3.12	498	7.99	25.6	3.1	39	47.00	41.63	5.37	89	94.31
LZ2	1,000	158645, 4180445	2.23	647	7.12	28.1	4.1	51	41.66	15.13	26.53	36	111.38
LZ3	1,200	158095, 4180445	1.93	799	12.99	30.8	6.6	97	59.32	0.29	59.03	0.5	193.61

[a] Abbreviations: E_h, redox potential; EC, electric conductivity; DO, dissolved oxygen; T, temperature. Iron species identification was performed *in situ* by colorimetric titration.
[b] The numbers correspond to (*X*, *Y*) universal transverse mercator (UTM) coordinates.

as well as their respective locations, are summarized in Tables 1 and 2. Previous studies had shown that highly anoxic and acidic water with a high concentration of iron in its reduced form emanates at a high temperature (ca. 31°C) from the mine portal (43). The first sample in this study was taken 20 m downstream (*LZ1*), with a dissolved oxygen of 39% saturation (equivalent to 3.1 mg/liter DO), a pH of 3.1, a temperature of 25.6°C, and a concentration of ferric iron of 300 mg/liter over a total iron concentration of 2.7 g/liter [89% $Fe(II)/Fe_{total}$]. At *LZ2*, the situation was completely different; the dissolved oxygen rose to 51% saturation (4.1 mg/liter DO), the total iron concentration was lower (~2.3 g/liter), and ferrous iron represented only 36% of the total iron content. The pH decreased to 2.2, and the temperature was around 28°C. Finally, at *LZ3*, the oxidation of Fe(II) was complete. Dissolved oxygen was near saturation (97% saturation, or 6.6 mg/liter DO), and total iron was around 3.3 g/liter, with only 1% ferrous iron. This station showed the lowest pH value (1.9), and the temperature was 30.8°C. The flow rate was around 0.8 liters/s at the origin and decreased rapidly due to evaporation. Specific conductivity also increased accordingly, from ~8 mS/cm at the source to ~13 mS/cm at *LZ3*, as a result of intense evaporation. These conductivity values correlate with the increase in the concentration of dissolved sulfate (the major anion in solution) and, to a lesser extent, with the increasing concentrations of some major cations such as Fe, Al, Mg, and Ca. The redox potential of the solution continuously increased, ascending from an initial value of 481 mV (characteristic of moderately reduced environments) at the mine portal to 800 mV (typical of fully oxidized mine waters [42]) in *LZ3*.

The sulfate and metal concentrations measured in the different sampling stations are summarized in Tables 1 and 2. The concentrations of sulfate and most metal cations (Al, Cu, Zn, and Ni, but also other conservative cations such as Na, Mg, and Ca, which are not shown in Table 2) increased downstream by a factor of around 2.1 to 2.5 as a consequence of evaporation. However, levels of other major cations and trace elements remained nearly constant (Cd and Co), increased only slightly (Fe), or exhibited sharp decreases (K, As, and Pb) along the studied segment. Given that the increase in concentration was an artifact produced by intense evaporation during the sampling period, the reported variations actually indicate that some elements behaved conservatively (Al, Mg, Ca, Na, Cu, Zn, and Ni), whereas others (e.g., Fe, K, As, Pb, Cd, and Co) were affected by hydrolysis or precipitation and coprecipitation processes to various extents.

With respect to metal toxicity, in addition to the metals reported above, significant concentrations of highly toxic elements such as U (up to 114 μg/liter), Tl (up to 51 μg/liter), and Cr (up to 28 μg/liter) were also measured (not shown), resulting in an increase in the overall toxicity of this acidic mine effluent.

Eukaryotic diversity. Most of the eukaryotic community was distributed in biofilms of different thicknesses all along the riverbed (Fig. 1A; see also Fig. S2 in the supplemental material). A total of 10 taxa were microscopically distinguished (Table 3), although, of these, only five were detected by molecular techniques. In *LZ1*, where the water column was light green due to the large amount of ferrous iron, the stream bed of the effluent was coated with a continuous photosynthetic biofilm (Fig. 1A). In this biofilm, species related to the Chlorophyta genus *Chlorella* dominated the phytobenthic community (Table 3). Additionally, species related to the genera *Pinnularia* (diatom), *Chlamydomonas* (green algae), *Vahlkampfia* (amoeba), *Actinophrys* (heliozoa), *Bodo* (flagellate), and *Oxytricha* (ciliate) were also detected at this location. Between sampling stations *LZ1* and *LZ2* the water column turned red, since the ferric iron concentration increased from ca. 0.3 to 1.5 g/liter. The phototrophic biofilms disappeared and were replaced by iron-precipitated sediments. At site *LZ2*, where the water was orange, some sporadic photosynthetic filamentous biofilms were found (Fig. 1C; see also Fig. S3 in the supplemental material). Filamentous algae, represented by the genus *Zygnemopsis*, were the dominant species, although *Chlamydomonas*, *Pinnularia*, and *Euglena* species were also present in smaller numbers at this location. At the *LZ3* station, where the iron was 99% oxidized (Table 1), phototrophic biofilms were smaller and scattered (Fig. 1E; see also Fig. S4 in the supple-

TABLE 2. Chemical analyses of water samples from the three sampling stations along La Zarza-Perrunal effluent

Sample	Distance from origin (m)	Major metal content			Trace metal or metalloid content			
		Al (mM)	Cu (mM)	Zn (mM)	Ni (μM)	Cd (μM)	Co (μM)	As (μM)
LZ1	20	12.79	0.32	0.86	1.40	54.17	13.17	30.06
LZ2	1,000	15.01	0.39	1.01	1.30	55.52	16.78	<5
LZ3	1,200	29.50	0.70	1.85	1.36	62.60	33.69	<5

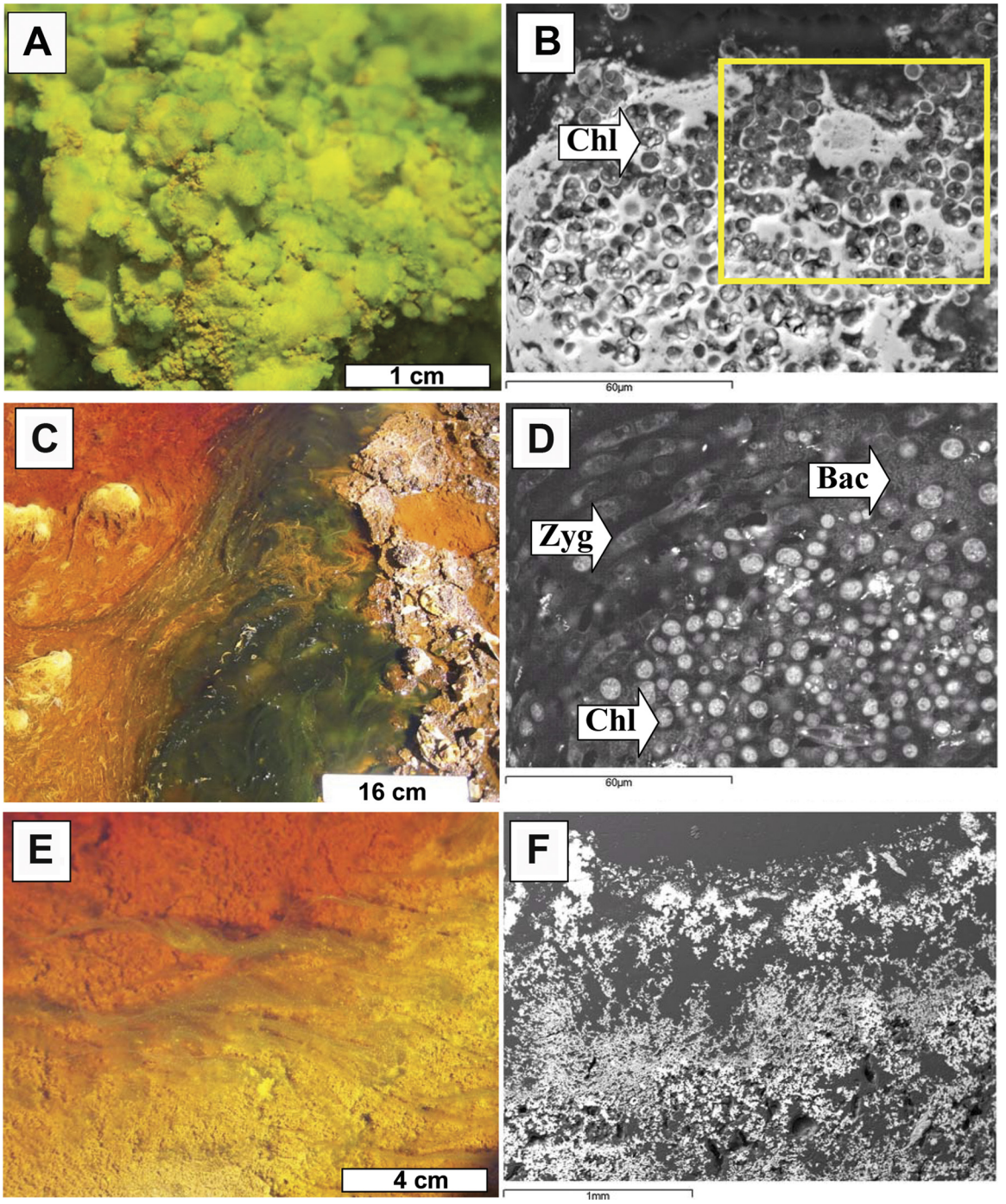

FIG. 1. Macroscopic and ultrastructure photographs of the different biofilms found in *LZ1*, *LZ2*, and *LZ3*. (A) General view of the *Chlorella* biofilms present at 20 m from the source. The yellowish areas are where schwertmanite starts to precipitate onto the biofilms. (B) SEM-BSE image of the *Chlorella* (Chl) biofilms with mineral precipitates around the cells (arrow). (C) General view of the floating filamentous algae (*Zygnemopsis*) present at 1,000 m from the source. (D) SEM-BSE image of the floating filamentous communities of *Zygnemopsis* (Zyg), showing the presence of associated *Chlorella* and bacterial (Bac) communities (arrows). (E) General view of the scarce communities present at 1,200 m from the source. The yellowish areas show where jarosite is more abundant. (F) SEM-BSE image of the structure of the sediments with porous layers of fine-grained minerals.

mental material). The main species detected was *Chlamydomonas* sp. The filamentous *Zygnemopsis* species and another *Chlorophyta* species related to the genus *Stichococcus* were also identified. Diatoms were represented by species of the genus *Pinnularia.* Additionally, although algae accounted for the greatest proportion of the biomass, there were other protozoan components present in low numbers such as species of *Ochromonas*.

TABLE 3. Eukaryotic community detected in Zarza-Perrunal effluent by different methodologies

Sampling site	Order	Family	Genus	Identification technique(s)[a]
LZ1	*Chlorellales*	*Chlorellaceae*	*Chlorella*	LM/16S plastid
	Volvocales	*Chlamydomonadaceae*	*Chlamydomonas*	LM
	Naviculales	*Pinnulariaceae*	*Pinnularia*	LM
	Stramenopiles	*Actinophryidae*	*Actinophrys*	LM
	Kinetoplastida	*Bodonidae*	*Bodo*	LM
	Sporadotrichida	*Oxytrichidae*	*Oxytricha*	LM
	Schizopyrenida	*Vahlkampfiidae*	*Vahlkampfia*	LM
LZ2	*Volvocales*	*Chlamydomonadaceae*	*Chlamydomonas*	LM/16S plastid
	Zygnematales	*Zygnemataceae*	*Zygnemopsis*	LM/16S plastid
	Naviculales	*Pinnulariaceae*	*Pinnularia*	LM/16S plastid
	Euglenales	*Euglenophyceae*	*Euglena*	LM
LZ3	*Volvocales*	*Chlamydomonadaceae*	*Chlamydomonas*	LM/16S plastid
	Zygnematales	*Zygnemataceae*	*Zygnemopsis*	LM/16S plastid
	Microthamniales	Not assigned	*Stichococcus*	LM
	Naviculales	*Pinnulariaceae*	*Pinnularia*	LM/16S plastid
	Ochomonadales	*Ochromonadaceae*	*Poteriochromonas*	16S plastid

[a] Abbreviations: LM, light microscopy; 16S plastid, 16S rRNA plastid cloning.

Microbial diversity. (i) Bacterial 16S rRNA gene clone libraries. A bacterial rRNA gene clone library was obtained from each sampling site. Sequences of bacterial 16S rRNA clones were compared with those available in the NCBI database by BLAST analysis. Of the 185 sequences analyzed with an average length of ≥1,400 bp, 13% were identified as chimeras or showed other irregularities and were not analyzed further. A total of 161 bacterial sequences were selected for phylogenetic analysis. The number of useful clones was higher in station *LZ1* and lower in station *LZ3*. The 71 analyzed clones from *LZ1* were grouped into 19 operational taxonomic units (OTUs) based on 97% sequence homology (Fig. 2; see also Table S1 in the supplemental material). The 56 clones from *LZ2* were grouped into 8 OTUs (Fig. 2; see also Table S2 in the supplemental material), and the 34 clones from *LZ3* were grouped into 8 OTUs (Fig. 2; see also Table S3 in the supplemental material).

The analysis of environmental clones showed that the bacterial communities consisted of various phylogenetic groups. The metabolic relationships of the different identified clones with the iron and sulfur cycles are indicated in the corresponding tables. Members of the *Alphaproteobacteria*, *Betaproteobacteria*, *Gammaproteobacteria*, *Nitrospira*, and *Actinobacteria* phyla were present at every sampling station. Additionally, members of the *Acidobacteria* and *Firmicutes* were present at *LZ1* and *LZ*3 and of the *Deltaproteobacteria* and *Planctomyces* at *LZ1*. The phylogenetic groups detected at the different stations are reported as supplemental data (see Tables S1, S2, and S3 in the supplemental material). Within the *Alphaproteobacteria*, the most abundant phylotypes were closely related to

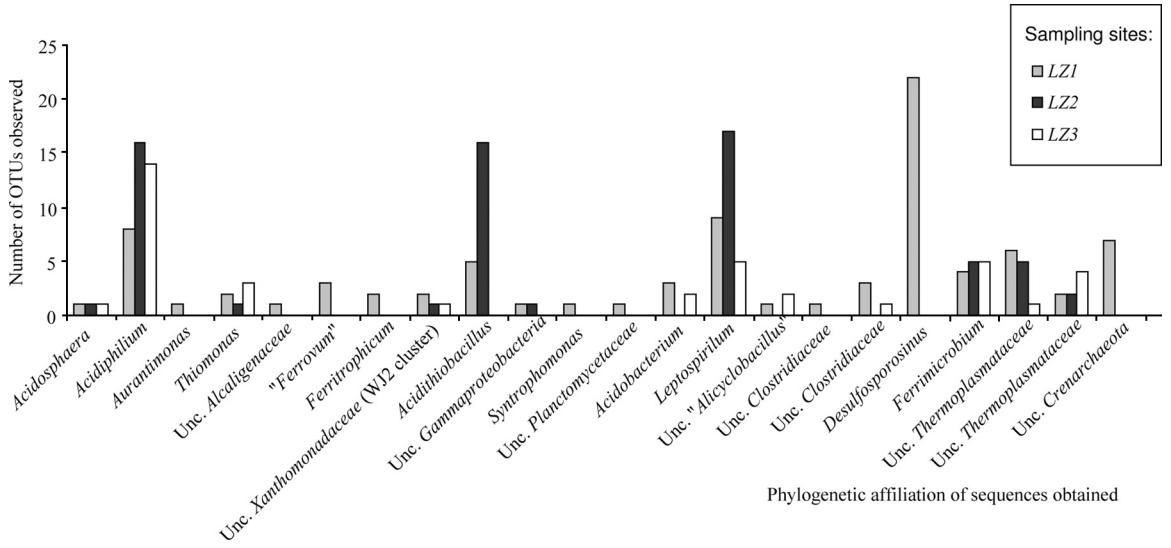

FIG. 2. Phylogenetic affiliations and OTUs observed. Phylogenetic affiliations of the sequences obtained at every station (*LZ1*, *LZ2*, and *LZ3*) are represented together with the numbers of OTUs observed for every phylotype. Unc., uncultured.

Acidiphilium (*A. crytum*, *A. angustum*, or uncultured *Acidiphilium* spp.), although some sequences clustered together with *Acidosphaera* (in *LZ1*, *LZ2*, and *LZ3*) or *Aurantimonas* (*LZ1*). A set of 6 sequences from the three stations clustered together with members of the genus *Thiomonas* from the *Betaproteobacteria*. Additionally, six sequences in *LZ1* were related to other *Betaproteobacteria*: *Ferritrophicum* (iron-oxidizing bacteria from a rhizosphera; DQ386263 [52]), *Alcaligenaceae* (uncultured clone AF232922), and an unclassified *Betaproteobacteria* ("*Ferrovum*" cluster; EF409840). With respect to *Gammaproteobacteria*, sequences clustering with unclassified *Xanthomonadaceae* species (WJ2 cluster; EF612418) were obtained in every library, and sequences related to the well-characterized acidophilic bacterium *Acidithiobacillus ferrooxidans* appeared only in *LZ1* and *LZ2*. Regarding *Deltaproteobacteria*, only one sequence related to *Syntrophobacter* was detected in *LZ1*. Sequences clustering with species of the *Nitrospira* phylum (*Leptospirillum ferridiazotrophum* and *Leptospirillum ferrooxidans*) were identified in the three sampling sites. Concerning the *Actinobacteria* phylum, related sequences were obtained in every station. All these sequences were related to strains or uncultured *Actinomycetales* species isolated and detected in AMD or Río Tinto, an extreme environment with a rather constant acidic pH along 92 km of river and a high concentration of heavy metals (2, 3, 4, 5, 6, 17, 18, 29, 49), such as species of *Ferromicrobium* and other phylogenetically close uncultured bacteria. Sequences related to *Acidobacteria* species identified in *LZ1* and *LZ3* clustered with uncultured bacteria detected in acidic soils, AMD, or Río Tinto. Regarding *Firmicutes*, sequences related to bacilli and clostridia were detected in stations *LZ1* and *LZ3*; the sequences of the bacilli were particularly similar to those of *Alicyclobacillus*. A total of 26 *Clostridium* sequences in both stations were similar to those of several uncultured species of *Clostridiaceae*, and 22 sequences showed similarity to the sulfate-reducing bacterium *Desulfosporosinus* sp. Finally, one sequence obtained from *LZ1* was related to an uncultured *Planctomycetes* (DQ906078) species isolated from soil in the Río Tinto banks.

(ii) Archaeal 16S rRNA gene clone libraries. Sequences belonging to the *Archaea* domain were found at every sampling site (Fig. 2; see also Tables S1, S2, and S3 in the supplemental material). At all three stations, sequences related to the *Euryarchaeota* phylum were obtained, and in *LZ1*, seven sequences were assigned to the *Crenarchaeota*. In all cases, the closest relatives for *Euryarchaea* sequences, specifically, uncultured archaea related to acid environments (EF396244, EF396245, EF396246, AF523936, EU370308, and DQ303248), were assigned to the *Thermoplasmata* class. For *Crenarchaeota*, all clones were related (99% similarity) to uncultured archaea from soil associated with trembling aspen (EF021659) and other uncultured archaea from soils.

(iii) Eukaryotic plastid 16S rRNA gene clone libraries. Sequences with similarity to the eukaryotic plastids were found at every sampling site (Table 3). At all three stations, sequences related to the genus *Chlorella* were obtained. Furthermore, in *LZ2* and *LZ3*, sequences related to the genera *Chlamydomonas*, *Pinnularia*, *Zygnemopsis*, and *Poteriochromonas* were also detected.

SEM-BSE study of the ultrastructure of the community in photosynthetic biofilms. Macroscopically, the first part of the stream at the *LZ1* sampling location was covered by a dense *Chlorella* biofilm (Fig. 1A). When SEM-BSE was used in the visualization of sections of this material, it was possible to observe how the *Chlorella* cells were surrounded by hydrous iron oxide precipitates (Fig. 1B). Previous X-ray diffraction analyses (42, 43) indicated that the hydrous iron oxides consisted mostly of schwertmannite, and EDS digital mapping of sulfur and iron indicated that this hydroxysulfate of iron with very low crystallinity was surrounding the *Chlorella* cells and the areas with bacterial biofilms. As a result, the iron terraces in the first section of the stream were formed by the precipitation of schwertmannite on the biofilms. Both the algae and bacteria previously present on the biofilms were preserved as a cast in the precipitated material (see Fig. S2 in the supplemental material).

At the *LZ2* sampling area, the biofilm communities were least abundant, and an increase in the floating communities of filamentous green algae *Zygnemopsis* was observed (Fig. 1C). There were also chlamydomonas and bacteria associated to filamentous green algae, although they did not form biofilms such as were seen in the stream sediments (Fig. 1D). These filamentous floating communities were covered by schwertmannite. The precipitation of schwertmannite in this case was associated not only with the cell surfaces but also with the extracellular substances surrounding the cells. The minerals precipitated around the floating communities also showed nucleation around bacterial cells and preservation of their presence as a cast in the minerals. In this area it was possible to observe the precipitation and formation of very thin films of schwertmannite on the surface of the filamentous algae (see Fig. S3 in the supplemental material).

Macroscopically and microscopically, the iron terraces at *LZ3*, the last sampling point, commonly presented a rough lamination consisting of thin, dense, and wavy laminae and thicker, porous, sponge-like layers (Fig. 1E). Morphological and EDS elemental analysis indicated alternate schwertmannite and jarosite precipitations, in correlation with previous XRD results (42, 43). As shown by scanning electron microscopy, the schwertmannite formed very fine spherulite-shaped particles that were commonly aggregated, forming a poorly cohesive layer (Fig. 1F), whereas jarosite had a more crystalline character (see Fig. S4 in the supplemental material).

Most of the filamentous green algae and their associated bacteria and microalgae are present floating in the water (Fig. 1C and E); thus, they do not play an important role in the formation of iron terraces in the sediments, although the presence of the organic surfaces helps trap and nucleate some minerals present in the waters (see Fig. S4 in the supplemental material) and contributes to the formation of the terraces after the organisms decay, as shown in Fig. S3 in the supplemental material.

The transition observed from the purely schwertmannitic to the mixed schwertmannitic-jarositic character of the ferric precipitates from *LZ1* to *LZ3* agrees with geochemical calculations carried out for the different sampling points (see Fig. S5 in the supplemental material). Thus, the saturation index values obtained for different Fe(III) minerals indicate that, at *LZ1*, schwertmannite precipitation is favored over other phases such as jarosite or goethite precipitation (saturation index values are positive and comparable, but schwertmannite

shows much faster precipitation kinetics). Conversely, the formation of jarosite is increasingly favored with increasing distance (schwertmannite becomes undersaturated as the pH decreases from 3.1 to around 2 in *LZ2* and *LZ3*). The development of these iron terraces resulting from the precipitation of Fe(III) hydroxysulphates around microbial cells has been also observed and discussed in a study of the adjacent Tintillo river (45).

DISCUSSION

Geochemical parameters. The rapid oxidation of Fe(II) and the subsequent hydrolysis of Fe(III), with precipitation of poorly crystallized minerals such as schwertmannite at pH 2 to 3, constitutes an efficient mechanism of natural attenuation which considerably reduces the transfer of mining-related pollutants (especially Fe and As and, to a lesser extent, Pb) to rivers and water reservoirs. The hydrolysis and precipitation of bacterially oxidized iron result in the release of acidity and the lowering of pH and also promote the formation of abundant mineral colloids that have a very high specific surface area and act as efficient sorbents for certain trace elements. Samples of schwertmannite collected from this area and analyzed in a previous study (43) were reported to exhibit very high concentrations of As and Cd, which supports the assumption that these elements have been significantly adsorbed by the ochreous precipitates.

Overall, among the most important physicochemical variations observed in the present study, there is one that is clearly related to the observed changes in the microbial communities. It is the rapid transition from anoxic conditions and ferrous iron-dominated conditions to oxygen-saturated and highly oxidizing conditions, where ferric iron is the dominant redox species in solution. Thus, the redox chemistry of iron resulting from the microbial processes discussed in the next section determines the geochemical evolution of the acidic effluent.

Microbial ecology model. The changes in the microbial diversity of this effluent were mainly determined by analysis using an oxygen gradient. Within the mine portal, conditions are anoxic, so in the first section of the effluent the microorganisms involved in the various chemical reactions must be anaerobic (obligate or facultative) sulfur- and iron-reducing microorganisms (12, 19). At the *LZ1* station, the presence of oxygen generated by the photosynthetic biofilms, together with the atmospheric oxygen diffusing throughout the water column, favors the appearance of iron- and sulfur-oxidizing microorganisms (Fig. 2; see also Table S1 in the supplemental material). This might have affected the level of prokaryotic diversity detected at this point, which was the highest level found in the analyzed effluent.

Further downstream, the increase in levels of oxygen and the oxidizing reactions led to an increase in ferric iron and a concomitant increase in the level of E_h. The hydrolysis and precipitation of ferric iron (in the form of schwertmannite and/or jarosite) led to a decrease in pH. As a result, much lower microbial diversity was detected at *LZ2* and *LZ3*. This gradient is also reflected in the water's color. Near the mine portal, where most of the iron is reduced (88% in *LZ1*), the water had a transparent greenish color. Downstream, the iron was oxidized and the water became orange and, further on, reddish. At *LZ3*, where 99% of the iron is oxidized, the water was deep red. This $Fe(II)/Fe_{total}$ gradient could be linked to the changes in eukaryotic diversity. Most of the eukaryotic biomass is located in the first part of the effluent, where iron is reduced and water transparent. Photosynthetic biofilms in this area had no problem capturing light. Where the water turned red due to iron oxidation and the formation of colloidal precipitates, the light intensity was drastically attenuated and the photosynthetic biofilms were sporadic and located in the shallower areas of the effluent. This phenomenon has been observed in other AMD and in Río Tinto, where ferrous iron-rich waters present a high eukaryotic biomass level (3, 24, 40).

The transition of photosynthetic biofilms can also be clearly shown by ultrastructural analysis using SEM-BSE. As a result of the geochemical transition, levels of precipitates increased along the effluent. This increase in mineral precipitation might be responsible for the decrease in eukaryotic diversity along the effluent. *Chlorella* was the predominant genus in *LZ1*, where iron was reduced, and *Zygnemopsis* sp. was the main photosynthetic organism where iron was oxidized (Table 3). A possible explanation could be that species of *Zygnemopsis* are filamentous algae that can float on water surfaces, facilitating the capture of radiation. In any case, due to the increase in levels of ferric iron and the corresponding precipitates at the lower part of the effluent, even the *Zygnemopsis* communities are affected, causing them to appear sporadically. In previous studies, high concentrations of iron and the resulting iron oxide deposition have been reported as inhibitors of algal development on stream substrata (11, 53). Other studies of iron-enriched streams indicated that bacteria also play an important role in deterring the development of algal communities (48). A similar transition of biofilm communities in acidic streams in Río Tinto was previously described (5).

Once the main microorganisms thriving in the Zarza-Perrunal effluent were identified, a model for the microbial ecology based on the physicochemical gradient observed in this effluent was developed. The bacterial and archaeal assemblages found in this ecosystem seem to be dominated by species mainly involved in the sulfur and iron cycles (Fig. 2; see also Tables S1, S2, and S3 in the supplemental material). Near the portal (*LZ1*), where sequences related to sulfate-reducing microorganisms of genera such as *Desulfosporosinus* and *Syntrophomonas* have been detected together with iron-reducing bacteria of the *Acidiphilium*, unclassified *Xanthomonas*, *Acidobacterium*, *Acidosphaera*, and *Clostridium* genera, the low concentration of dissolved oxygen favors sulfur and iron reduction metabolisms. The identification of microorganisms such as *Acidithiobacillus ferrooxidans*, a species of the genus *Ferrimicrobium*, that are able to oxidize or reduce iron depending on the presence or absence of oxygen suggests an increase in the levels of opportunistic microorganisms able to obtain energy under the variable redox conditions of the water column. The identification of iron-oxidizing species of the *Leptospirillum* and "*Ferrovum*" genera, and of sulfur oxidizers, such as the previously mentioned *Acidithiobacillus ferrooxidans* and *Thiomonas* spp., underlines the existence of a vertical gradient of redox conditions at this site that results from the activity of photosynthetic algae and the diffusion of atmospheric oxygen. Downstream, from *LZ2* to *LZ3*, sulfate-reducing microorgan-

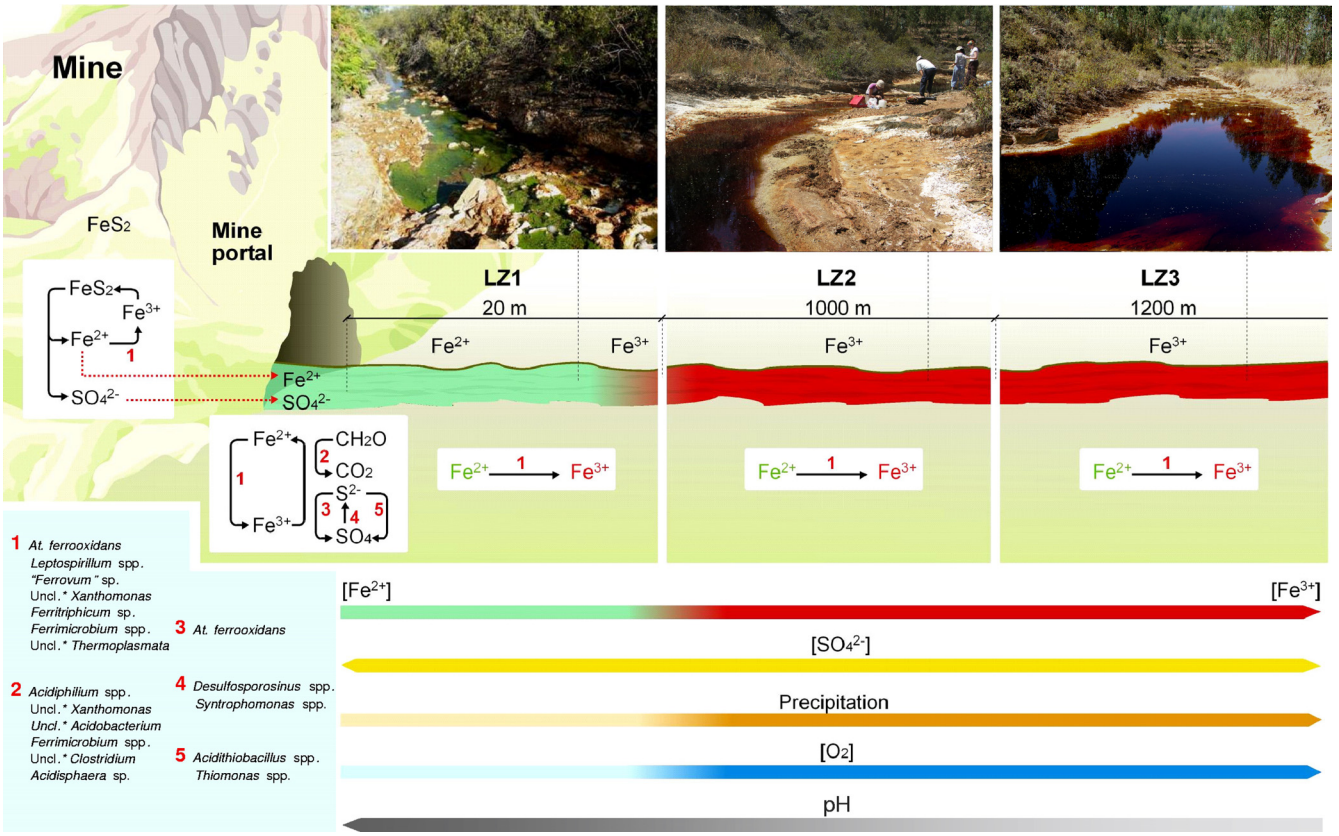

FIG. 3. A basic geomicrobiological scheme for the Zarza-Perrunal effluent. Microorganisms are shown associated with their roles in the iron and sulfur cycles. The font sizes of the names of the organisms are proportional to their respective cell numbers. Uncl.*, unclassified.

isms were not detected and iron-oxidizing microorganisms such as *Leptospirillum* spp. were the dominant detected clones.

Some facultative microorganisms were present in the three analyzed stations of the effluent, for example, members of the *Acidiphilium* or the *Ferrimicrobium* genera. These bacterial groups consist of obligate or facultative heterotrophic species normally associated with extreme acidic environments (9, 24). In general, they are very versatile microorganisms that are able to adapt to different conditions (24). For example, they can use ferric iron for anaerobic respiration in anoxic conditions and, in the case of some species of *Acidiphilium*, also in microaerobic and oxic conditions (24). This versatility allows these species to thrive along the length of the effluent in spite of the changes in the environmental conditions. It is widely accepted that organic compounds are toxic for obligate chemolithotrophic acidophiles (21). A potential ecological role of these heterotrophic bacteria might be that of biodegradation of these toxic organic compounds, thereby facilitating growth of the more sensitive chemolithotrophic microorganisms (23).

The versatility of *Acidithiobacillus ferrooxidans* allows its metabolic activity to use reduced sulfur compounds as an energy source and ferric iron as an electron acceptor in the anoxic section of the effluent and ferrous iron as an energy source along with oxygen as an electron acceptor in the oxic part (31). However, this species was identified only in stations *LZ1* and *LZ2*; it was not detected at *LZ3.* This could have been due to the high concentration of ferric iron present at *LZ3* (22). It is well established that other iron-oxidizing bacteria like *Leptospirillum* spp., also present in *LZ3*, can displace *Acidithiobacillus ferrooxidans*, because the former is more resistant to extreme conditions (38, 46, 47). *Leptospirillum* spp. can tolerate lower pH and higher ferric iron concentrations and temperatures than species of *Acidithiobacillus*. *LZ3* showed the highest temperature and highest iron concentration and the lowest pH of all the sampling stations (38, 46).

With respect to archaea, species of *Thermoplasmatales*, which are common in extreme acidic environments, were present all along the effluent (15, 18, 24). The metabolic versatility of the members of this order enables them to thrive in the three analyzed stations. The presence of species of *Crenarchaeota* in *LZ1* is more puzzling, as the sequences detected are not related to acidophilic archaeal sequences. The most closely related sequences were derived from an iron-rich soil (20) and from a soil associated with trembling aspen (28). In future studies, other *Archaea*- or *Crenarchaeota*-specific primers could be used to determine the presence of members of these phyla in this ecosystem and other AMD.

Photosynthetic eukaryotes play a fundamental role in this ecosystem due to their autotrophy, especially in the first section of the effluent (*LZ1*), where the eukaryotic biomass abounds. In addition to the diffusion of atmospheric oxygen along the stream, the oxygen produced by the photosynthetic organisms must favor the aerobic oxidation of iron and sulfur and the subsequent microbial transition described above.

Figure 3 shows a basic geomicrobiological scheme for the Zarza-Perrunal effluent that takes into account the physiological properties of the identified microorganisms. The transition between anoxic and oxic conditions and its influence on the iron redox state can be correlated with the microbial diversity and the known metabolic properties of the identified microorganisms. Although similar schemes have been described for Río Tinto and other AMD (18, 24), the size and the complexity of those ecosystems, especially in the case of the Tinto basin, impede the study of clear transitions such as those detected in this work. In addition, the iron terraces produced by the precipitation of Fe(III) hydroxysulphates around microbial cells have not been studied in other extreme acidic systems. They have been observed and described in a study of the adjacent Tintillo river (45), but in this case, the microbial diversity was not analyzed.

These results are extremely important for bioleaching and bioremediation processes. It is clear that oxygen is the limiting factor for the formation of a high concentration of ferric iron, which is the oxidizing agent required for efficient bioleaching operations. Furthermore, the generation of anoxic conditions favors the activity of iron-reducing microorganisms, which can further reduce the effective concentration of ferric iron and as a result decrease the efficiency of bioleaching. Anoxic conditions also favor the activity of sulfate-reducing microorganisms that generate H_2S and might sequester soluble metals by precipitating metal sulfides. Additionally, the generation of reduced iron could favor an increase in the pH, leading to the formation of iron precipitates that are able to sequester bioleached metals. These results are important observations that have to be considered in the design of heap-leaching processes to ensure an efficient extraction of metals of economical value. From the bioremediation point of view, realizing the possibility of elimination toxic metals from industrial effluents would require knowledge and control of the different biological processes promoting precipitation, sorption, and redissolution of metals. The particular geomicrobial characteristics of La Zarza-Perrunal effluent should allow the evaluation of all these factors of environmental and biotechnological interest in a small, manageable and affordable area of study.

ACKNOWLEDGMENTS

We thank Marina Postigo for DNA sequencing and Marta Diez Ercilla for sampling support.

A.A. and V.S.-E. were supported by a Ramón y Cajal contract from the Ministerio de Educación y Ciencia. E.G.-T. is supported by Instituto Nacional de Tecnica Aeroespacial (INTA). This work has been supported by grants from the MICINN-Spain (CGL2008-02298/BOS) and the Centro de Astrobiología (CSIC-INTA).

REFERENCES

1. **Achenbach, L., and C. Woese.** 1995. 16S and 23S rRNA-like primers, p. 521–523. *In* K. R. Sower and H. J. Schreier (ed.), Archaea: a laboratory manual. Cold Spring Harbor Laboratory Press, Cold Spring Harbor, NY.
2. **Aguilera, A., F. Gómez, E. Lospitao, and R. Amils.** 2006. A molecular approach to the characterization of the eukaryotic communities of an extreme acidic environment: methods for DNA extraction and denaturing gradient gel electrophoresis analysis. Syst. Appl. Microbiol. **29:**593–605.
3. **Aguilera, A., S. C. Manrubia, F. Gómez, N. Rodríguez, and R. Amils.** 2006. Eukaryotic community distribution and its relationship to water physicochemical parameters in an extreme acidic environment, Río Tinto (southwestern Spain). Appl. Environ. Microbiol. **72:**5325–5330.
4. **Aguilera, A., V. Souza-Egipsy, F. Gómez, and R. Amils.** 2007. Development and structure of eukaryotic biofilms in an extreme acidic environment, Río Tinto (SW Spain). Microb. Ecol. **53:**294–305.
5. **Aguilera, A., et al.** 2007. Distribution and seasonal variability in the benthic eukaryotic community of Río Tinto (SW Spain), an acidic, high metal extreme environment. Syst. Appl. Microbiol. **30:**531–546.
6. **Amaral Zettler, L. A., et al.** 2002. Eukaryotic diversity in Spain's River of Fire. Nature **417:**137.
7. **Ascaso, C., and J. Wierzchos.** 1994. Structural aspects of the lichen-rock interface using back-scattered electron imaging. Bot. Acta **107:**251–256.
8. **Ashelford, K. E., N. A. Chuzhanova, J. C. Fry, A. J. Jones, and A. J. Weightman.** 2006. New screening software shows that most recent large 16S rRNA gene clone libraries contain chimeras. Appl. Environ. Microbiol. **72:**5734–5741.
9. **Bond, P. L., G. K. Druschel, and J. F. Banfield.** 2000. Comparison of acid mine drainage microbial communities in physically and geochemically distinct ecosystems. Appl. Environ. Microbiol. **66:**4962–4971.
10. **Bourrelly, P.** 1966. Les algues d'eau douce. Initiation à la systématique. Éditions N. Boubée y Cie, Paris, France.
11. **Chon, H. T., and J. H. Hwang.** 2000. Geochemical characteristics of the acidic mine drainage in the water system in the vicinity of the Dogye coal mine in Korea. Environ. Geochem. Health **22:**155–172.
12. **Coupland, K., and D. B. Johnson.** 2008. Evidence that the potential for dissimilatory ferric iron reduction is widespread among acidophilic heterotrophic bacteria. FEMS Microbiol. Lett. **279:**30–35.
13. **Davis, C. C.** 1955. The marine and freshwater plankton. Michigan State University, East Lansing, MI.
14. **DeLong, E. F.** 1992. *Archaea* in coastal marine environments. Proc. Natl. Acad. Sci. U. S. A. **89:**5685–5689.
15. **Edwards, K. J., P. L. Bond, T. M. Gihring, and J. F. Banfield.** 2000. An archaeal iron-oxidizing extreme acidophile important in acidic mine drainage. Science **287:**1796–1798.
16. **Ehrlich, H. L., and D. K. Newman.** 2009. Geomicrobiology, 5th ed. Tayor and Francis Group, Boca Raton, FL.
17. **García-Moyano, A., E. Gonzalez-Toril, A. Aguilera, and R. Amils.** 2007. Prokaryotic community composition and ecology of floating macroscopic filaments from an extreme acidic environment, Río Tinto (SW Spain). Syst. Appl. Microbiol. **30:**601–614.
18. **Gonzalez-Toril, E., E. Llobet-Brossa, E. O. Casamayor, R. Amann, and R. Amils.** 2003. Microbial ecology of an extreme acidic environment, the Tinto River. Appl. Environ. Microbiol. **69:**4853–4865.
19. **Hallberg, K. B., and D. B. Johnson.** 2001. Biodiversity of acidophilic prokaryotes. Adv. Appl. Microbiol. **49:**37–84.
20. **Hansel, C. M., S. Fendorf, P. M. Jardine, and C. A. Francis.** 2008. Changes in bacterial and archaeal community structure and functional diversity along a geochemically variable soil profile. Appl. Environ. Microbiol. **74:**1620–1633.
21. **Harrison, J. A. P.** 1984. The acidophilic thiobacilli and other acidophilic bacteria that share their habitat. Annu. Rev. Microbiol. **38:**265–292.
22. **Huber, T., G. Faulkner, and P. Hugenholtz.** 2004. Bellerophon: a program to detect chimeric sequences in multiple sequence alignments. Bioinformatics **20:**2317–2319.
23. **Johnson, B. D., and K. B. Hallberg.** 2003. The microbiology of acidic mine waters. Res. Microbiol. **154:**466–473.
24. **Johnson, B. D., and K. B. Hallberg.** 2009. Carbon, iron and sulfur metabolism in acidophilic micro-organisms. Adv. Microb. Physiol. **54:**201–255.
25. **Lane, D. J.** 1991. 16S/23S rRNA sequencing, p. 115–175. *In* E. Stackebrandt and M. Goodfellow (ed.), Nucleic acid techniques in bacterial systematics. John Wiley & Sons, Chichester, United Kingdom.
26. **Lee, J. L., S. H. Hutner, and E. C. Bovee.** 1985. An illustrated guide to the protozoa. Allen Press, Lawrence, KS.
27. **Leedale, G. F.** 1967. Euglenoid flagellates (Concepts of Modern Biology series). Prentice-Hall Inc., Englewood Cliffs, NJ.
28. **Lesaulnier, C., et al.** 2008. Elevated atmospheric CO_2 affects soil microbial diversity associated with trembling aspen. Environ. Microbiol. **10:**926–941.
29. **López-Archilla, A. I., I. Marín, and R. Amils.** 2001. Microbial community composition and ecology of an acidic aquatic environment: the Tinto River, Spain. Microb. Ecol. **41:**20–35.
30. **Ludwig, W., et al.** 2004. ARB: a software environmental for sequence data. Nucleic Acids Res. **32:**1363–1371.
31. **Malki, M., et al.** 2006. Importance of the iron cycle in biohydrometallurgy. Hydrometallurgy **83:**223–228.
32. **Margesin, R., and F. F. Schinner.** 2001. Potential of halotolerant and halophilic microorganisms for biotechnology. Extremophiles **5:**73–83.
33. **Margulis, L., J. O. Corliss, M. Melkonian, and D. J. Chapman.** 1990. Handbook of *Protoctista.* Jones and Barlett Publishers, Boston, MA.
34. **Niehaus, F., C. Bertoldo, M. Kähler, and G. Antranikian.** 1999. Extremophiles as a source of novel enzymes for industrial application. Appl. Microbiol. Biotechnol. **51:**711–729.
35. **Nordstrom, D. K., and C. N. Alpers.** 1999. Geochemistry of acid mine waters, p. 133–160. *In* G. S. Plumlee and M. J. Logsdon (ed.), The environmental geochemistry of mineral deposits, part A: processes, techniques, and health issues. The Society of Economic Geologists, Littleton, CO.
36. **Pinedo Vara, I.** 1961. Piritas de Huelva (su historia, minería y aprovechamiento). Summa, Madrid, Spain.

37. **Rawlings, D. E., and D. B. Johnson.** 2007. The microbiology of biomining: development and optimization of mineral-oxidizing microbial consortia. Microbiology **153:**315–324.
38. **Rawlings, D. E., H. Tributsch, and G. S. Hansford.** 1999. Reasons why '*Leptospirillum*'-like species rather than *Thiobacillus ferrooxidans* are the dominant iron-oxidizing bacteria in many commercial processes for the biooxidation of pyrite and related ores. Microbiology **145:**5–13.
39. **Round, F. E., R. M. Crawford, and D. G. Mann.** 1990. The diatoms: biology and morphology of the genera. Cambridge University Press, Cambridge, United Kingdom.
40. **Rowe, O. F., J. Sánchez España, K. B. Hallberg, and D. B. Johnson.** 2007. Microbial communities and geochemical dynamics in an extremely acidic, metal-rich stream at an abandoned sulfide mine (Huelva, Spain) underpinned by two functional primary production systems. Environ. Microbiol. **9:**1761–1771.
41. **Russell, N. J.** 2000. Toward a molecular understanding of cold activity of enzymes from psychrophiles. Extremophiles **4:**83–90.
42. **Sánchez España, J., et al.** 2005. Acid mine drainage in the Iberian Pyrite Belt (Odiel River watershed, Huelva, SW Spain): geochemistry, mineralogy and environmental implications. Appl. Geochem. **20:**1320–1356.
43. **Sánchez España, J., E. López Pamo, E. Santofimia Pastor, J. Reyes Andrés, and J. A. Martín Rubí.** 2005. The natural attenuation of two acidic effluents in Tharsis and La Zarza-Perrunal mines (Iberian Pyrite Belt, Huelva, Spain). Environ. Geol. **49:**253–266.
44. **Sánchez España, J., E. López-Pamo, E. Santofimia, J. Reyes, and J. A. Martín Rubí.** 2007. The oxidation of ferrous iron in acidic mine effluents from the Iberian Pyrite Belt (Odiel Basin, Huelva, Spain): field and laboratory rates. J. Geochem. Explor. **92:**120–132.
45. **Sánchez España, J., E. Santofimia, and E. López-Pamo.** 2007. Iron terraces in acid mine drainage systems: a discussion about the organic and inorganic factors involved in their formation through observations from the Tintillo acidic river (Riotinto mine, Huelva, Spain). Geosphere **3:**133–151.
46. **Sand, W., K. Rohde, B. Sobotke, and C. Zenneck.** 1992. Evaluation of *Leptospirillum ferrooxidans* for leaching. Appl. Environ. Microbiol. **58:**85–92.
47. **Schrenk, M. O., K. J. Edwards, R. M. Goodman, R. J. Hamers, and J. F. Banfield.** 1998. Distribution of *Thiobacillus ferrooxidans* and *Leptospirillum ferrooxidans*: implications for generation of acid mine drainage. Science **279:**1519–1522.
48. **Sheldon, S. P., and T. A. Wellnitz.** 1998. Do bacteria mediate algal colonization in iron-enriched streams? OIKOS **83:**85–92.
49. **Souza-Egipsy, V., et al.** 2008. Prokaryotic community structure in algal photosynthetic biofilms from extreme acidic streams in Río Tinto (Huelva, Spain). Int. Microbiol. **11:**251–260.
50. **Tell, G., and V. Conforti.** 1986. *Euglenophyta* pigmentadas de la Argentina. Bibliotheca Phycologica, Berlin, Germany.
51. **van Geen, A., J. F. Adkins, E. A. Boyle, C. H. Nelson, and A. Palenques.** 1997. A 120-year record of widespread contamination from mining of the Iberian Pyrite Belt. Geology **25:**291–294.
52. **Weiss, J., et al.** 2007. Characterization of neutrophilic Fe(II)-oxidizing bacteria isolated from the rhizosphere of wetland plants and description of *Ferritrophicum radicicola* gen. nov. sp. nov. and *Sideroxydans paludicola* sp. nov. Geomicrobiol. J. **24:**559–570.
53. **Wellnitz, T. A., and S. P. Sheldon.** 1995. The effect of iron and manganese colonization on diatom colonization in a Vermont stream. Freshwater Biol. **34:**465–470.
54. **Wierzchos, J., and C. Ascaso.** 1994. Application of back-scattered electron imaging to the study of the lichen-rock interface. J. Microsc. **175:**54–59.